

Exclusive pion radiative capture from nuclei in the Δ region

Frank X.-D. Lee and L. E. Wright

Physics Department, Institute of Nuclear and Particle Physics, Ohio University, Athens, Ohio 45701

C. Bennhold

Department of Physics, Center for Nuclear Studies, George Washington University, Washington, D.C. 20052

(Received 13 December 1993)

Calculations are presented for the exclusive pion radiative capture reaction from complex nuclei $A(\pi, \gamma N)B$ in the framework of the nonlocal distorted wave impulse approximation. Our results are found to be in reasonable agreement with a recent TRIUMF experiment $^{16}\text{O}(\pi^+, \gamma p)^{15}\text{O}$. Since pion radiative capture is related to pion photoproduction via time reversal invariance, the findings reported here are at variance with the recent BATES experiment $^{16}\text{O}(\gamma, \pi^- p)^{15}\text{O}$.

PACS number(s): 25.80.Hp, 25.20.Lj

In a recent paper we developed the formalism for calculating quasifree exclusive pion photoproduction on complex nuclei [1]. Since the final nucleon is in a continuum state, this reaction provides large kinematic flexibility and reduces the sensitivity to nuclear structure. Our computations were performed in a distorted wave impulse approximation (DWIA) framework carried out in either coordinate or momentum space. Previous descriptions [2,3] were developed in coordinate space only where the momentum dependencies of the operator were either neglected or approximated. While our calculations gave reasonable agreement with data for the reaction $^{12}\text{C}(\gamma, \pi^- p)^{11}\text{C}$ taken at Tomsk, we had serious discrepancies with forward pion data but not with backward pion data from a recent BATES experiment $^{16}\text{O}(\gamma, \pi^- p)^{15}\text{O}$ [3].

Pion radiative capture accompanied by single nucleon emission is closely related to quasifree pion photoproduction and, therefore, can access the same physics questions. The same ingredients, such as the elementary amplitude, shell model bound state wave functions, and optical potentials for the nucleon and pion can be used in both reactions. Consequently, one would expect to reproduce the experimental data of both or neither of the two processes. This comparison has been successfully employed [4] in pion photoproduction and radiative capture on p -shell nuclei without nucleon emission, namely, $^{13}\text{C}(\gamma, \pi^-)^{13}\text{N}_{\text{g.s.}}$ and $^{13}\text{C}(\pi^+, \gamma)^{13}\text{N}_{\text{g.s.}}$. After introducing additional 2p-2h components in the ground state wave function of the $A=13$ system, the combined data set for both processes could be adequately described. This relationship has also been used by Reynaud and Tabakin in their study of $^{15}\text{N}(\pi^+, \gamma)^{15}\text{O}_{\text{g.s.}}$ [5].

The interplay between pion photoproduction and radiative capture may become even more important when it is accompanied by nucleon knockout since the presence of the continuum nucleon opens up essentially all the angular momentum channels of the reaction. While the matrix elements for the capture process $A(\pi, \gamma N)B$ are identical to those of the photoproduction process $B(\gamma N, \pi)A$ by time reversal invariance, we are interested in $A(\pi^+, \gamma p)B$ and $A(\gamma, p\pi^-)B$ which are not directly related by time reversal invariance. However, the basic reactions $n(\pi^+, \gamma)p$ and $p(\gamma, \pi^+)n$ are related by time reversal invariance. Thus, if we allow the

target nucleon to be in the continuum and the final nucleon to be bound, we can use time reversal invariance to evaluate the pion radiative capture cross section using matrix elements for the photoproduction process. The radiative capture nuclear cross section is then obtained by including appropriate kinetic factors in the calculation. The presence of different projectiles in the initial or final state can be taken into account with the use of realistic optical potentials.

In the laboratory frame the target is at rest and the incoming pion beam defines the z axis while the photon is produced in the x - z plane with $\phi_\pi = 0^\circ$. Let the four momenta of the pion, struck nucleon, photon, outgoing nucleon, initial nucleus, and residual nucleus be $q^\mu = (E_\pi, \mathbf{q})$, $p_i^\mu = (p_i^0, \mathbf{p}_i)$, $k^\mu = (E_\gamma, \mathbf{k})$, $p^\mu = (E_N, \mathbf{p})$, $P_i^\mu = (M_i, \mathbf{0})$, $P_f^\mu = (E_f, \mathbf{Q})$, respectively. Following standard procedures, the differential cross section for $A(\pi, \gamma N)B$ in the laboratory frame can be written as

$$d\sigma = \frac{1}{2E_\pi} \frac{M_i}{E_i} \frac{M_f d\mathbf{Q}}{E_f (2\pi)^3} \frac{d\mathbf{k}}{2E_\gamma (2\pi)^3} \frac{m_N d\mathbf{p}}{E_N (2\pi)^3} \times \overline{\sum} |M_{fi}^{(\pi, \gamma)}|^2 (2\pi)^4 \delta^{(4)}(q^\mu + P_i^\mu - P_f^\mu - k^\mu - p^\mu) \quad (1)$$

where $M_{fi}^{(\pi, \gamma)}$ denotes the transition matrix element for the pion radiative capture reaction and $\overline{\sum}$ denotes the sum over final spins and average over initial spins and the delta function ensures overall energy-momentum conservation. In the impulse approximation, the momentum of the struck nucleon is equal to the negative of the momentum transfer, $\mathbf{p}_i = -\mathbf{Q}$. After integrating over the momentum transfer \mathbf{Q} and the magnitude of the outgoing nucleon momentum $|\mathbf{p}|$, we obtain the threefold coincidence differential cross section:

$$\frac{d^3\sigma}{dE_\gamma d\Omega_\gamma d\Omega_N} = \frac{M_f m_N |\mathbf{k}| |\mathbf{p}|}{4(2\pi)^5 E_\pi |E_N + E_f + E_N \mathbf{p} \cdot (\mathbf{k} - \mathbf{q}) / p^2|} \times \overline{\sum} |M_{fi}^{(\pi, \gamma)}|^2. \quad (2)$$

In the impulse approximation the matrix element squared reduces to a sum over single particle matrix element given by

$$\begin{aligned} \overline{\sum} |M_{fi}^{(\pi, \gamma)}|^2 &= \overline{\sum} |M_{fi}^{(\gamma, \pi)}|^2 \\ &= \frac{1}{(2J_i + 1)} \sum_{\alpha \lambda m_s} \frac{S_\alpha}{2j + 1} |T^{(\gamma, \pi)}(\alpha, \lambda, m_s)|^2 \end{aligned} \quad (3)$$

where J_i is the spin of the target, $\alpha = \{nljm\}$ are the quantum numbers of the bound nucleon, λ is the photon polarization label, m_s is the spin projection of the outgoing nucleon, and S_α is the spectroscopic factor. Note we have used the fact that the matrix elements $M_{fi}^{(\pi, \gamma)} = M_{fi}^{(\gamma, \pi)}$ due to time reversal invariance. The single particle matrix element for pion photoproduction is given by

$$\begin{aligned} T^{(\gamma, \pi)}(\alpha, \lambda, m_s) &= \int d^3r \phi_\pi^{(+)}(\mathbf{r}, -\mathbf{q}) \Psi_\alpha^\dagger(\mathbf{r}) \\ &\quad \times t_{\gamma\pi}(\lambda, \mathbf{k}, \mathbf{p}_i, \mathbf{q}, \mathbf{p}) \Psi_{m_s}^{(+)}(\mathbf{r}, \mathbf{p}) e^{i\mathbf{k} \cdot \mathbf{r}} \end{aligned} \quad (4)$$

where $\mathbf{p}_i = \mathbf{p} + \mathbf{k} - \mathbf{q}$ is the momentum of the bound nucleon. We note that this matrix element describes pion photoproduction on a continuum nucleon while the nucleon in the final state is bound. In momentum space the same matrix element is given by

$$\begin{aligned} T^{(\gamma, \pi)}(\alpha, \lambda, m_s) &= \int d^3p' d^3q' \phi_\pi^{(+)}(\mathbf{q}', \mathbf{q}) \Psi_\alpha^\dagger(\mathbf{p}_i) \\ &\quad \times t_{\gamma\pi}(\lambda, \mathbf{k}, \mathbf{p}_i, \mathbf{q}', \mathbf{p}') \Psi_{m_s}^{(+)}(\mathbf{p}', \mathbf{p}) \end{aligned} \quad (5)$$

with $\mathbf{p}_i = \mathbf{p}' + \mathbf{k} - \mathbf{q}'$. Working in momentum space allows a straightforward treatment of all nonlocal effects arising from the production operator without any approximation. However, the price we pay is the evaluation of a six-dimensional integral which requires considerable numerical computation. On the other hand, performing this integration numerically and thus avoiding angular momentum recoupling facilitates applying our formalism to the radiative pion capture reaction by simply interchanging the continuum nucleon from the final to the initial state. Procedures for evaluating Eqs. (4) and (5) with various levels of approximation are discussed in Ref. [1].

Figure 1 shows the kinematic arrangement of the TRIUMF experiment in the laboratory frame. The experiment was done with positive pion beams of two energies, $T_\pi = 160$ and 220 MeV, incident on a ^{16}O target; the emitted photons and protons are detected in coincidence in a coplanar geometry at two photon angles, one forward ($\theta_\gamma = 77.4^\circ$), one backward ($\theta_\gamma = 125.4^\circ$); and, for each photon angle, at four proton angles on the other side of the pion beam, $\theta_p = 15.7^\circ, 28.7^\circ, 41.7^\circ, 54.7^\circ$. The resulting differential cross sections are presented as a function of the photon energy E_γ . Since the energy resolution was not sufficient to resolve the $p_{1/2}$ and $p_{3/2}$ hole states of the residual nucleus ^{15}O , the data represent the combined cross sections for the capture of pions by p -shell neutrons in the ^{16}O target.

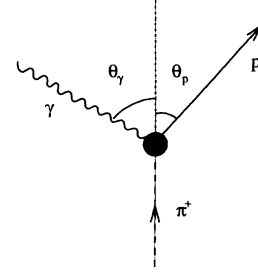


FIG. 1. Kinematic arrangement of the TRIUMF experiment in the laboratory frame.

In Fig. 2 we show the individual contributions from the Born background and the resonant Δ excitation for one of the kinematic situations of the experiment. It is the coherent interference of the two that gives rise to the final cross sections. One can see that the role of the Δ contribution becomes more dominant compared to the Born contribution as the proton angle increases. This can be understood by looking at W , the invariant mass of the outgoing γp pair. For photon energies between 100 to 335 MeV, W ranges from 1137 to 1233 MeV, 1155 to 1235 MeV, 1181 to 1238 MeV, 1214 to 1242 MeV, corresponding to the four proton angles in increasing order. Therefore, increasing the proton angle moves the peak of the Δ more into the invariant mass range. The change in the shape of the distributions can be attributed to the following two factors. The first one is related to the nuclear momentum transfer Q , while the second one can be understood from the interference between the Born and Δ contributions. Let us examine the first factor in more detail. The momentum transfer Q is equal in magnitude to the bound nucleon momentum. It is the momentum distribution of the bound nucleon wave function that is largely responsible for the shapes of the excitation function. In the photon energy range, $E_\gamma = 100$ to 335 MeV, Q has the following behavior. For $\theta_p = 15.7^\circ$, we have $Q = 391$ MeV/c at $E_\gamma = 100$ MeV, the momentum transfer then decreases to reach a minimum of 185 MeV/c around $E_\gamma = 260$ MeV. After that Q rises again to 342 MeV/c at $E_\gamma = 335$ MeV. Since the struck neutron is in the p shell, this minimum explains the peak in the cross section. For the next proton angle, $\theta_p = 28.7^\circ$, the relevant values for Q become 401, 100, and 330 MeV/c at the same photon energies. Since the p -shell neutron momentum distribution has a maximum around 100 MeV/c, the cross section peaks at this value. For $\theta_p = 41.7^\circ$, the Q values are 440 MeV/c at $E_\gamma = 100$ MeV, 100 MeV/c at $E_\gamma = 235$ MeV, reaching its minimum of 20 MeV/c at $E_\gamma = 265$ MeV, 100 MeV/c again at $E_\gamma = 295$ MeV, and finally 322 MeV/c at $E_\gamma = 335$ MeV. For the largest proton angle, $\theta_p = 54.7^\circ$, the corresponding Q values are 495, 144, 70, 100, and 320 MeV/c at the same photon energies as in the previous case. Crossing $Q = 100$ MeV/c twice provides an explanation for the double peak structure in the latter two cases. It also explains the single peaks in the first two cases because Q crosses 100 MeV/c only once. To understand the different heights in the peaks, we have to turn to the interference between the background and the resonance. In case of a constructive interference, we obtain the higher peak, while destructive interference leads to a lower peak.

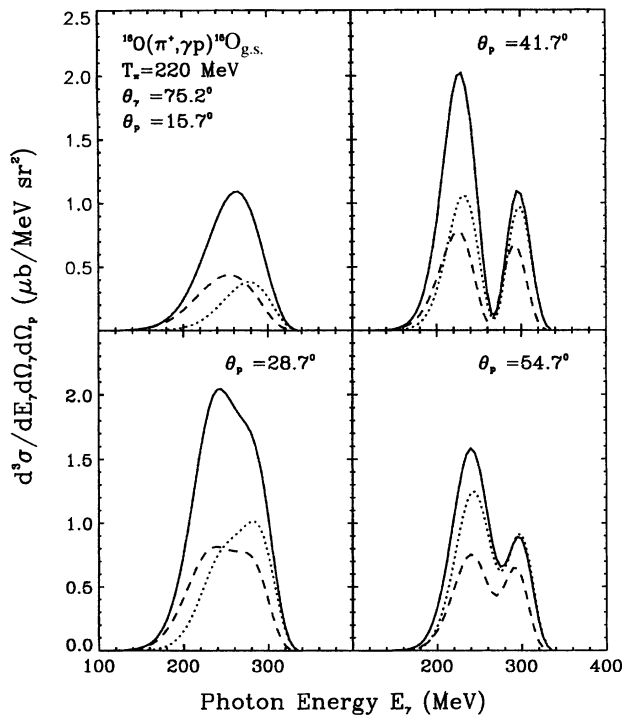


FIG. 2. Contributions from the Born (dashed curves) and Δ (dotted curves) terms to the coincidence cross sections of the reaction $^{16}\text{O}(\pi^+, \gamma p)^{15}\text{O}_{\text{g.s.}}$ as functions of the outgoing photon energy E_γ are shown for four outgoing proton angles $\theta_p = 15.7^\circ, 28.7^\circ, 41.7^\circ, 54.7^\circ$ at incident pion energy $T_\pi = 220$ MeV and photon angle $\theta_\gamma = 75.2^\circ$. The solid curves are the coherent sum of the two. The calculations are done in PWIA.

In Fig. 3 we demonstrate the distortion effects resulting from the pion-nucleus interaction in the initial state and the proton-nucleus interaction in the final state for two typical cases. Clearly, distortion effects are significant and reduce the plane wave impulse approximation (PWIA) cross section by a factor of 3 to 4 which is larger than the amount of distortion found in the photoproduction reaction. Most of the reduction is due to pion distortion since the pion energy is in the Δ region where strong absorption occurs. Note that the shape of the peaks is somewhat smeared out by the final state interactions. In these calculations, we used the pion optical potential by Stricker, McManus, and Carr [7] and the proton optical potential by Schwandt [8]. To investigate sensitivities to the optical potentials, we also employed the pion optical potential by Gmitro, Kamalov, and Mach [9] and the proton optical potential by Cooper, Hama, Clark, and Mercer [10]. The results varied by less than 15% around the peaks.

In Fig. 4 we present a comparison of our predictions with preliminary data from TRIUMF for $T_\pi = 220$ MeV and $\theta_\gamma = 75.2^\circ$. The overall agreement is fairly good, and distortions play an important role in obtaining the correct normalization. Nonlocal effects are rather small judging from the few points that we have calculated. We point out that there are no free parameters in the calculation we have performed. All model ingredients have been fixed by other independent studies.

In Ref. [1] our theoretical calculation was shown to give

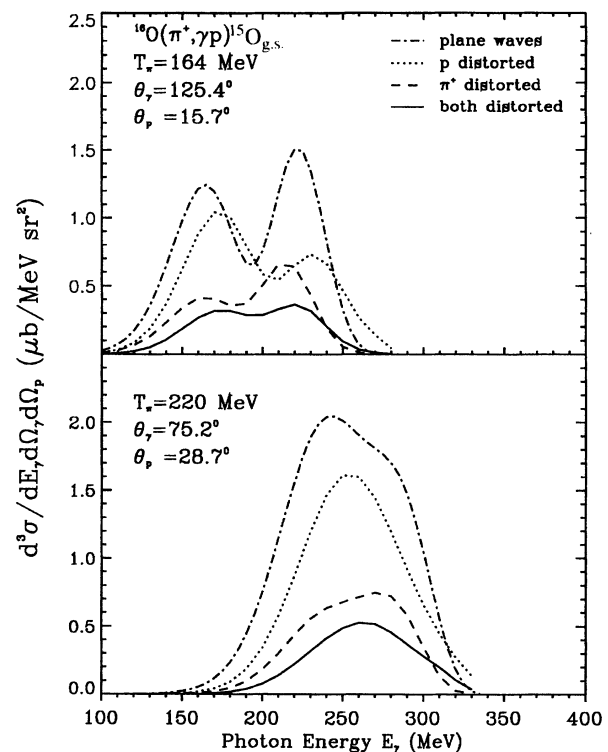


FIG. 3. The pion and proton distortion effects for two different kinematic cases in the experiment.

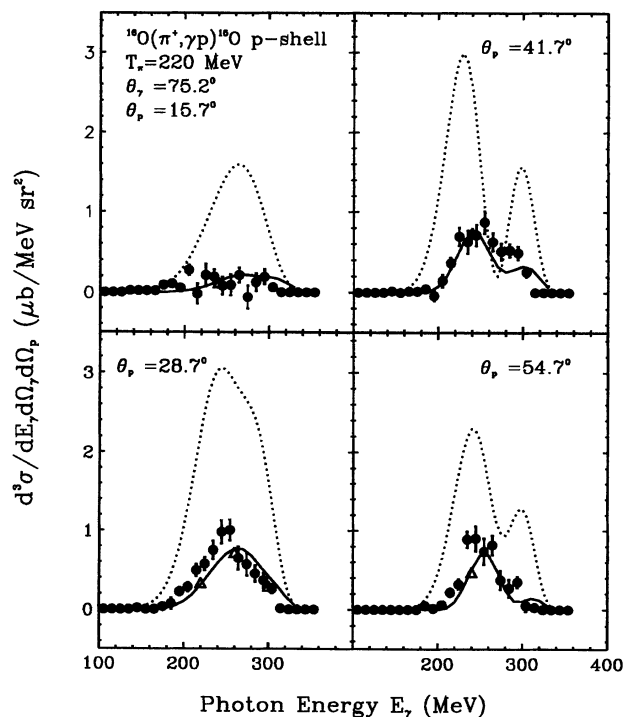


FIG. 4. The combined cross sections from $p_{1/2}$ and $p_{3/2}$ neutrons in ^{16}O are compared to the data from TRIUMF [6]. The dashed curves are our predictions in PWIA, the solid curves in local DWIA, and the triangle (Δ) in nonlocal DWIA.

satisfactory agreement with data from Tomsk. However, we overpredicted recent BATES data at forward pion angle by about a factor of 3. Our $(\gamma, \pi N)$ results were recently confirmed by an independent calculation [11] in a Δ -hole approach. Their computation demonstrates that the Δ -hole results are close to our DWIA calculation and, therefore, cannot account for the observed discrepancy. The $\theta_p = 28.7^\circ$ case in Fig. 4 corresponds to pion photoproduction at 75.2° . Therefore, the good description achieved here suggests that the results of the BATES experiment are not compatible with the new TRIUMF data.

It should be mentioned that so far data are available only for this one set of kinematics. There are three more sets of data with different pion energies and photon angles which are currently being analyzed. We have made predictions for these cases and the results await the analysis.

In conclusion, we have performed the first calculation for the exclusive pion radiative capture reaction $A(\pi, \gamma N)B$ in a nonlocal DWIA approach. The excitation functions of the differential cross section can be understood in the impulse approximation. The interference between the Born back-

ground and the Δ resonant contribution is found to be important. Distortion due to pion-nucleus and nucleon-nucleus interactions plays a significant role and attenuates the PWIA cross section by about a factor of 3. Our predictions are in reasonable agreement with data from a recent TRIUMF experiment $^{16}\text{O}(\pi^+, \gamma p)^{15}\text{O}$. Since pion radiative capture and pion photoproduction are related by time reversal invariance, the results suggest that the BATES experiment and TRIUMF experiment are in contradiction with each other. A new experimental proposal [12] for another $^{16}\text{O}(\gamma, \pi^- p)^{15}\text{O}$ measurement has already been approved at NIKHEF in order to reexamine the earlier BATES data.

We thank Dr. D. Mack for releasing the data to us before publication. We also thank the Ohio Supercomputer Center for time on the Cray Y-MP. The work of F.X.L. and L.E.W. was supported in part by U.S. DOE under Grant No. FG02-87ER40370 and the work of C.B. under Grant No. FG05-86ER40270. A NATO Collaborative Research Grant is also gratefully acknowledged.

-
- [1] Xiaodong Li, L. E. Wright, and C. Bennhold, *Phys. Rev. C* **48**, 816 (1993).
 [2] J. M. Laget, *Nucl. Phys.* **A194**, 81 (1972).
 [3] L. D. Pham *et al.*, *Phys. Rev. C* **46**, 621 (1992).
 [4] C. Bennhold and L. Tiator, *Nucl. Phys.* **A519**, 805 (1990); *Phys. Lett. B* **238**, 31 (1990).
 [5] G. W. Reynaud and F. Tabakin, *Phys. Rev. C* **23**, 2652 (1981).
 [6] TRIUMF experiment 550 (unpublished), spokesperson, D. Mack (private communication).
 [7] K. Stricker, H. McManus, and J. A. Carr, *Phys. Rev. C* **19**, 929 (1979); **22**, 2043 (1980); **25**, 952 (1982).
 [8] P. Schwandt *et al.*, *Phys. Rev. C* **26**, 55 (1982).
 [9] M. Gmitro, S. S. Kamalov, and R. Mach, *Phys. Rev. C* **36**, 1105 (1987).
 [10] E. D. Cooper, S. Hama, B. C. Clark, and R. L. Mercer, *Phys. Rev. C* **47**, 297 (1993).
 [11] T. Sato and T. Takaki, *Nucl. Phys.* **A562**, 673 (1993).
 [12] NIKHEF proposal, spokesperson, G. von der Steenhoven.